Journal of Fluids and Structures (1997) **11,** 225–246

ANALYSIS AND COMPUTATION OF NONLINEAR DYNAMIC RESPONSE OF A TWO-DEGREE-OF-FREEDOM SYSTEM AND ITS APPLICATION IN AEROELASTICITY

B. H. K. Lee
Institute for Aerospace Research, National Research Council, Ottawa, Ontario, Canada

L. Gong and Y. S. Wong
Department of Mathematical Sciences, University of Alberta, Edmonton, Alberta, Canada

(Received 30 January 1996 and in revised form 21 August 1996)

This paper investigates the dynamic response of a coupled two-degree-of-freedom system with a cubic stiffness nonlinearity in both degrees of freedom. The mathematical model is based on a coupled system of Duffing's equations. The governing equations are derived for a two-dimensional airfoil oscillating in pitch and in plunge, but they can be applied to nonaeronautical problems, such as mechanical systems, by discarding the aerodynamics terms and setting the appropriate parameters to correspond to those for the particular dynamic system under consideration. Only the harmonic solution is considered and we use the method of slowly varying amplitude to investigate the dynamic response of the system to an external excitation. The equilibrium points are computed and a linear analysis is carried out to determine the stability of the equilibrium points. Examples are given for a dynamic system without aerodynamic forces to illustrate the complex structure of the jump phenomenon where the solution jumps from one branch of the amplitude-frequency curve to the other. An example in aeroelasticity is given which shows the behaviour of the airfoil motion as the velocity approaches the linear flutter speed. Numerical simulations are also carried out to verify the analytical results.

1 INTRODUCTION

In aeroelastic investigations of aircraft, we usually assume that the structural behaviour of aircraft components is linear (Bisplinghoff *et al.* 1955; Fung 1969). However, in reality nonlinearities are present in one form or the other. Structurally, they may occur in the restoring forces and can be treated as nonlinear springs for example, springs with free-play, hysteresis or cubic nonlinearities. These types of nonlinearities have been investigated by Woolston *et al.* (1957) for a two-dimensional airfoil performing pitching and plunging motions using an analog computer. There are serious drawbacks in the use of an analog computer to study nonlinear flutter, and accuracy is often not as high as we would desire in order to investigate the characteristics of the airfoil motion fully.

An alternate approach was suggested by Shen (1959) using the well-known Kryloff & Bogoliuboff (1947) method in nonlinear vibration theory. The original limitation of weak nonlinearities can be removed by adopting a modification given by Popov (1957). The analysis assumes the existence of a periodic solution dominated by the fundamental harmonic. The amplitude of oscillation in the degree of freedom which contains the nonlinearity is prescribed, and the critical velocity at which the specified oscillation

0889–9746/97/030225 + 22 $25.00/fl960075

will be sustained is then determined. However, it has not been demonstrated how large the magnitude of the nonlinearities is admissible and how the effects of initial conditions on the flutter boundary can be accounted for.

For a one-degree-of-freedom system with cubic restoring force in the absence of aerodynamic loads, Jones & Lee (1985) investigated the multi-valued response curve of amplitude versus frequency and showed the effects of initial conditions on the steady state of the system under forced oscillations. Lee & LeBlanc (1986) and Lee & Desrochers (1987) expanded the numerical technique developed by Jones & Lee (1985) and describe a method for nonlinear flutter analysis that eliminates the limitations inherent in the earlier methods (Woolston *et al.* 1957; Shen 1959) by the use of a time-marching finite-difference scheme. Using incompressible aerodynamics, the aeroelastic equations for a two-dimensional airfoil performing plunging and pitching motions are written as a pair of simultaneous finite difference equations. The effect of initial conditions on nonlinear flutter was studied numerically by varying the displacement from equilibrium of the pitch angle at the start of the airfoil motion. More detailed studies were later carried out by Price *et al.* (1994, 1995) who computed power spectral densities, phase-space plots, Poincaré maps and Lyapunov exponents of the airfoil response to investigate the possibility of occurrence of chaos for certain airfoil parameters.

In this study, we concentrate on the harmonic solution of a coupled two-degree-of-freedom system with a cubic stiffness nonlinearity in both degrees of freedom. The method of slowly varying amplitude is employed to analyse the harmonic response. This results in an autonomous system of first-order nonlinear differential equations in a 12-dimensional phase-space. A stable equilibrium point of the resultant system gives one harmonic solution for the original system of equations. Linear analysis is then carried out to determine the stability of the equilibrium point. The analysis demonstrates that similarly to a one-degree-of-freedom system, a jump phenomenon from one steady state to another may occur for certain system parameters and range of the excitation frequency and amplitude. The amplitude response curve as a function of excitation frequency has a much more complicated structure than the corresponding one-degree-of-freedom system. Numerical integrations are used to verify the results obtained from the theoretical analysis and they also reveal some interesting dynamical features. Subharmonic solutions may exist under certain conditions, and these have been investigated numerically by Wong *et al.* (1995).

2. THEORETICAL ANALYSIS

2.1. Equations of Motion of a Nonlinear Coupled Two-Degree-of-Freedom System with Aerodynamic Forces

In this section, we investigate the harmonic response of a two-degree-of-freedom system with a cubic spring nonlinearity in both degrees of freedom. We choose for our system a two-dimensional airfoil oscillating in pitch and in plunge. The equations of motion derived can readily be adapted to other nonaeronautical systems, such as coupled mechanical systems, by neglecting the aerodynamics terms and setting the appropriate parameters to correspond to the particular dynamic system under consideration. It is well known that for a nonlinear system the output oscillations may have the same or different frequencies than the input excitation when the amplitude of the forcing function is varied. For a harmonic response, we restrict the output oscillation to have the same frequency as the input excitation force.

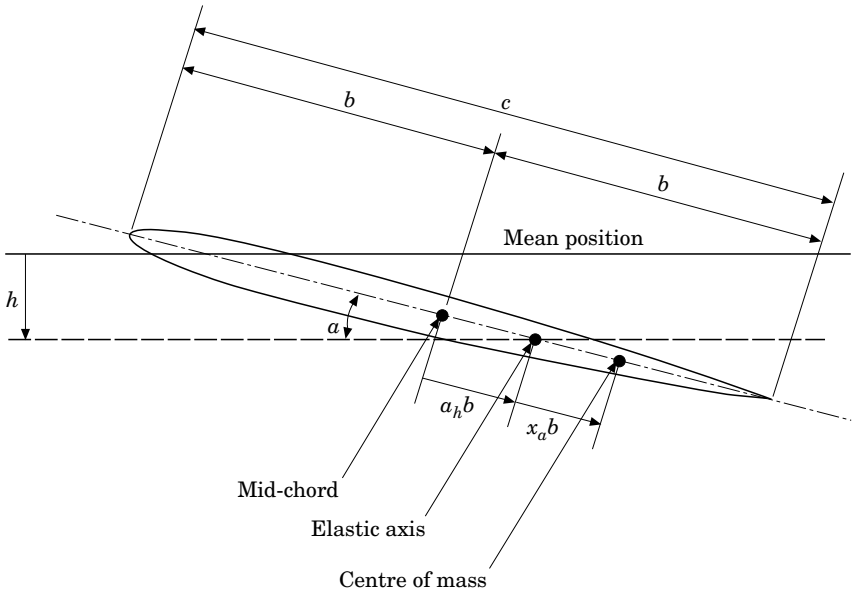

Figure 1. Two-degree-of-freedom airfoil motion.

Figure 1 shows the notations used in the analysis of a two-degree-of-freedom motion of an airfoil oscillating in pitch and in plunge. The plunging deflection is denoted by h, positive in the downward direction, α is the pitch angle about the elastic axis, positive with the nose up. The elastic axis is located at a distance $a_h b$ from the midchord, while the mass centre is located at a distance $x_\alpha b$ from the elastic axis. Both distances are positive when measured towards the trailing edge of the airfoil. The aeroelastic equations of motion for linear springs have been derived by Fung (1969). For nonlinear restoring forces such as those for cubic springs considered in this paper, they can be written as follows:

$$\xi'' + x_\alpha \alpha'' + 2\zeta_\xi \frac{\bar{\omega}}{U^*} \xi' + \left(\frac{\bar{\omega}}{U^*}\right)^2 (\xi + \beta_\xi \xi^3) = p(\tau), \tag{1}$$

$$\frac{x_\alpha}{r_\alpha^2} \xi'' + \alpha'' + 2\frac{\zeta_\alpha}{U^*} \alpha' + \frac{1}{U^{*2}} (\alpha + \beta_\alpha \alpha^3) = r(\tau), \tag{2}$$

where $\xi = h/b$ is the nondimensional displacement and the prime denotes differentiation with respect to the nondimensional time τ, defined as

$$\tau = \frac{Ut}{b}. \tag{3}$$

In equations (1) and (2), $\bar{\omega}$ is given by

$$\bar{\omega} = \frac{\omega_\xi}{\omega_\alpha}, \tag{4}$$

where ω_ξ, ζ_ξ, ω_α and ζ_α are the uncoupled plunging- and pitching-mode natural

frequencies and damping ratios, respectively, r_α is the radius of gyration about the elastic axis, β_ξ and β_α are the nonlinear spring constants, U^* is defined as

$$U^* = \frac{U}{b\omega_\alpha}, \tag{5}$$

and

$$p(\tau) = -\frac{1}{\pi\mu} C_L(\tau) + \frac{P(\tau)b}{mU^2}, \qquad r(\tau) = \frac{2}{\pi\mu r_\alpha^2} C_M(\tau) + \frac{Q(\tau)}{mU^2 r_\alpha^2} \tag{6}$$

in which $C_L(\tau)$ and $C_M(\tau)$ are the lift and pitching moment, respectively. $P(\tau)$ and $Q(\tau)$ are the external applied force and moment, m is the airfoil mass per unit length and μ is the airfoil–air mass ratio.

For incompressible flow, Fung (1969) gives the following expressions for $C_L(\tau)$ and $C_M(\tau)$:

$$\begin{aligned} C_L(\tau) = {} & \pi(\xi'' - a_h\alpha'' + \alpha') + 2\pi\{\alpha(0) + \xi'(0) + (\tfrac{1}{2} - a_h)\alpha'(0)\}\phi(\tau) \\ & + 2\pi\int_0^\tau \phi(\tau - \sigma)(\alpha'(\sigma) + \xi''(\sigma) + (\tfrac{1}{2} - a_h)\alpha''(\sigma))\,\mathrm{d}\sigma, \end{aligned} \tag{7}$$

$$\begin{aligned} C_M(\tau) = {} & \pi(\tfrac{1}{2} + a_h)\{\alpha(0) + \xi'(0) + (\tfrac{1}{2} - a_h)\alpha'(0)\}\phi(\tau) \\ & + \pi(\tfrac{1}{2} + a_h)\int_0^\tau \phi(\tau - \sigma)\{\alpha'(\sigma) + \xi''(\sigma) + (\tfrac{1}{2} - a_h)\alpha''(\sigma)\}\,\mathrm{d}\sigma \\ & + \frac{\pi}{2} a_h(\xi'' - a_h\alpha'') - (\tfrac{1}{2} - a_h)\frac{\pi}{2}\alpha' - \frac{\pi}{16}\alpha'', \end{aligned} \tag{8}$$

where the Wagner function $\phi(\tau)$ is given by

$$\phi(\tau) = 1 - \psi_1 \mathrm{e}^{-\epsilon_1\tau} - \psi_2 \mathrm{e}^{-\epsilon_2\tau}, \tag{9}$$

and the constants $\psi_1 = 0{\cdot}165$, $\psi_2 = 0{\cdot}335$, $\epsilon_1 = 0{\cdot}0455$ and $\epsilon_2 = 0{\cdot}3$ are given by Jones (1940).

2.2. Amplitude-Frequency Relation for Harmonic Oscillation

We assume that the external applied forces are sinusoidal and without loss in generality, the excitation is only applied in the pitch degree of freedom. In this case, $P(\tau) = 0$ and we write

$$Q(\tau) = Q_0 \sin(\omega\tau) \tag{10}$$

and let

$$F = \frac{Q_0}{mU^2 r_\alpha^2}, \tag{11}$$

so that the second term in equation (6) for $r(\tau)$ becomes $F\sin(\omega\tau)$.

After introducing four new variables

$$\begin{aligned} w_1 &= \int_0^\tau \mathrm{e}^{-\epsilon_1(\tau-\sigma)}\alpha(\sigma)\,\mathrm{d}\sigma, \qquad w_2 = \int_0^\tau \mathrm{e}^{-\epsilon_2(\tau-\sigma)}\alpha(\sigma)\,\mathrm{d}\sigma, \\ w_3 &= \int_0^\tau \mathrm{e}^{-\epsilon_1(\tau-\sigma)}\xi(\sigma)\,\mathrm{d}\sigma, \quad w_4 = \int_0^\tau \mathrm{e}^{-\epsilon_2(\tau-\sigma)}\xi(\sigma)\,\mathrm{d}\sigma, \end{aligned} \tag{12}$$

equations (1) and (2) can be written as

$$c_0\xi'' + c_1\alpha'' + c_2\xi' + c_3\alpha' + c_4\xi + c_5\xi^3 + c_6\alpha + c_7w_1 + c_8w_2 + c_9w_3 + c_{10}w_4 = f(\tau), \quad (13)$$

$$d_0\xi'' + d_1\alpha'' + d_2\alpha' + d_3\alpha + d_4\alpha^3 + d_5\xi' + d_6\xi + d_7w_1 + d_8w_2 + d_9w_3 + d_{10}w_4 = g(\tau), \quad (14)$$

and the coefficients in these equations are given in Appendix A.

For large values of τ when transients are damped out and steady-state solutions are obtained, $f(\tau) = 0$. For sinusoidal external forces, we assume the plunge and pitch motion to be of the following form:

$$\xi(\tau) = a_1(\tau)\cos(\omega\tau) + b_1(\tau)\sin(\omega\tau), \quad \alpha(\tau) = a_2(\tau)\cos(\omega\tau) + b_2(\tau)\sin(\omega\tau). \quad (15)$$

Here a_i and b_i $(i = 1, 2)$ are assumed to be slowly varying functions in τ. The second time derivatives are considered to be small and neglected. This approach is often used in perturbation analysis (Jordan & Smith 1983). We write w_i $(i = 1, 2, 3, 4)$ as follows:

$$\begin{aligned} w_1 &= a_3(\tau)\cos(\omega\tau) + b_3(\tau)\sin(\omega\tau), & w_2 &= a_4(\tau)\cos(\omega\tau) + b_4(\tau)\sin(\omega\tau), \\ w_3 &= a_5(\tau)\cos(\omega\tau) + b_5(\tau)\sin(\omega\tau), & w_4 &= a_6(\tau)\cos(\omega\tau) + b_6(\tau)\sin(\omega\tau). \end{aligned} \quad (16)$$

From equations (12) we take the time derivative of w_i and obtain

$$\begin{aligned} w_1'(\tau) &= \alpha(\tau) - \epsilon_1 w_1(\tau), & w_2'(\tau) &= \alpha(\tau) - \epsilon_2 w_2(\tau), \\ w_3'(\tau) &= \xi(\tau) - \epsilon_1 w_3(\tau), & w_4'(\tau) &= \xi(\tau) - \epsilon_2 w_4(\tau). \end{aligned} \quad (17)$$

Note that $\xi^3(\tau)$ and $\alpha^3(\tau)$ can be written as

$$\begin{aligned} \xi^3(\tau) &= \tfrac{3}{4}r^2(a_1\cos(\omega\tau) + b_1\sin(\omega\tau)) + \{\text{higher harmonics in } 3\omega\tau\}, \\ \alpha^3(\tau) &= \tfrac{3}{4}R^2(a_2\cos(\omega\tau) + b_2\sin(\omega\tau)) + \{\text{higher harmonics in } 3\omega\tau\}, \end{aligned} \quad (18)$$

where

$$r^2 = a_1^2 + b_1^2, \qquad R^2 = a_2^2 + b_2^2.$$

Here r and R denote the amplitudes of ξ and α respectively. Assuming the higher harmonic terms in equations (18) to be small and upon substituting equations (15), (16) and (18) into (13), (14) and (17), we obtain a system of 12 first-order nonlinear ordinary differential equations after matching the coefficients of $\cos(\omega\tau)$ and $\sin(\omega\tau)$. The resulting equations in matrix form are given as:

$$A\mathbf{x}' = \mathbf{y}(\mathbf{x}), \quad (19)$$

where

$$A = \begin{bmatrix} H & 0 \\ 0 & I \end{bmatrix}, \quad H = \begin{bmatrix} c_2 & 2\omega c_0 & c_3 & 2\omega c_1 \\ -2\omega c_0 & c_2 & -2\omega c_1 & c_3 \\ d_5 & 2\omega d_0 & d_2 & 2\omega d_1 \\ -2\omega d_0 & d_5 & -2\omega d_1 & d_2 \end{bmatrix}, \quad I = \begin{bmatrix} 1 & 0 & \dots & 0 \\ 0 & 1 & \dots & 0 \\ \cdots & \cdots & \cdots & \cdots \\ 0 & \dots & 0 & 1 \end{bmatrix}, \quad (20)$$

$$\mathbf{x} = \{a_1, b_1, a_2, \dots, a_6, b_6\}^{\mathrm{T}}, \qquad \mathbf{y}(\mathbf{x}) = \{y_1(\mathbf{x}), y_2(\mathbf{x}) \dots y_{12}(\mathbf{x})\}^{\mathrm{T}}$$

Here I is an 8×8 identity matrix and $y_i(\mathbf{x})$ are given in Appendix B. Since the interest

is in the harmonic solutions of equations (1) and (2) to external sinusoidal excitations, periodicity condition is enforced by requiring that a_i and b_i are constants. The harmonic solutions of equations (13) and (14) are identified by the equilibrium points of the system of equations (19). Setting $a_i' = 0$ and $b_i' = 0$, we obtain a system of 12 nonlinear algebraic equations. In deriving the expressions for a_1, b_1, a_2, and b_2, equation (19) is first solved for $a_3, b_3, \ldots, a_6$, and b_6 which are then substituted into the expressions for a_1, b_1, a_2, and b_2 to give the following:

$$\begin{aligned} -m_1 a_1 + p_1 b_1 - n_1 a_2 + s_1 b_2 + q_1 r^2 b_1 &= 0, \\ p_1 a_1 + m_1 b_1 + s_1 a_2 + n_1 b_2 + q_1 r^2 a_1 &= 0, \\ -m_2 a_1 + p_2 b_1 - n_2 a_2 + (s_2 + q_2 R^2) b_2 - F &= 0, \\ p_2 a_1 + m_2 b_1 + n_2 b_2 + (s_2 + q_2 R^2) a_2 &= 0, \end{aligned} \tag{21}$$

where the coefficients $m_1, m_2,$ etc. are given in Appendix C.

A frequency–amplitude relation can be derived and is given by

$$(D_1^2 + D_2^2) R^2 - D_3^2 F^2 = 0, \tag{22}$$

where

$$\begin{aligned} D_1 &= m_1[m_2 n_2 + p_2(s_2 + q_2 R^2)] + (p_1 + q_1 r^2)[p_2 n_2 - m_2(s_2 + q_2 R^2)] - n_1(p_2^2 + m_2^2), \\ D_2 &= m_1[p_2 n_2 - m_2(s_2 + q_2 R^2)] - (p_1 + q_1 r^2)[m_2 n_2 + p_2(s_2 + q_2 R^2)] + s_1(p_2^2 + m_2^2), \\ D_3^2 &= [m_1 m_2 + (p_1 + q_1 r^2) p_2]^2 + [m_1 p_2 - (p_1 + q_1 r^2) m_2]^2, \end{aligned} \tag{23}$$

and

$$R^2 = \frac{m_1^2 + (p_1 + q_1 r^2)^2}{n_1^2 + s_1^2} r^2. \tag{24}$$

The basic relation between the amplitude (r and R) and frequency (ω) for the two-degree-of-freedom system governed by equations (1) and (2) are now represented by equations (22) and (24). Clearly, a jump phenomenon and a multi-valued amplitude-frequency relation can be observed for the coupled system. Substituting the definitions given in Appendices B and C into equations (22) and (24), we find that the resulting equation is a polynomial of degree 11 in r^2. Once the value of r is computed, then R can be determined from equation (24). For certain values of ω both equations admit multi-valued amplitudes. Using the values of r and R, the equilibrium points are then determined from equations (21).

2.3. Linear Stability Analysis

To study the linear stability of the system of equations given by equation (19) about the equilibrium point $\mathbf{x}_e$, we introduce a small perturbation in the form

$$\mathbf{x} = \mathbf{x}_e + \boldsymbol{\eta} e^{\lambda \tau}, \tag{25}$$

where $|\eta| \ll 1$. Substituting into equation (19), we obtain the following equation:

$$A(\boldsymbol{\eta}' + \lambda\boldsymbol{\eta})e^{\lambda\tau} = \mathbf{y}(\mathbf{x}_e + \boldsymbol{\eta}e^{\lambda\tau}). \tag{26}$$

The right-hand side of equation (26) is a nonlinear function which can be linearized using Taylor's expansion, such that

$$\mathbf{y}(\mathbf{x}_e + \boldsymbol{\eta}e^{\lambda\tau}) = \mathbf{y}(\mathbf{x}_e) + \mathbf{D}_x[\mathbf{y}(\mathbf{x}_e)]\boldsymbol{\eta}e^{\lambda\tau} + \mathcal{O}(|\eta|^2). \tag{27}$$

Define the Jacobian matrix $\mathbf{D}_x[\mathbf{y}(\mathbf{x}_e)] = \mathbf{J}_x$, and since $\mathbf{y}(\mathbf{x}_e) = 0$, we obtain from equation (26) the following:

$$\boldsymbol{\eta}' = [A^{-1}\mathbf{J}_x - \lambda I]\boldsymbol{\eta}. \tag{28}$$

The linear stability of $\mathbf{x}_e$ is determined by the characteristic equation

$$|A^{-1}\mathbf{J}_x - \lambda I| = 0, \tag{29}$$

and $\mathbf{x}_c$ is stable if $\mathrm{Re}(\lambda) < 0$ for all the roots.

3. RESULTS AND DISCUSSION

In Section 2, a coupled two-degree-of-freedom system with a cubic stiffness nonlinearity in both degrees of freedom is studied. The equations are derived using a physical model of an airfoil submerged in a moving medium. However, the analysis is applicable to other mechanical systems in a stationary medium, and the aerodynamic forces can be discarded by dropping the appropriate terms. We first investigate the motion of a one- and two-degree-of-freedom dynamic system and later give an example in aeroelasticity. In order to apply the analysis to systems in the absence of aerodynamic forces, we show the necessary modifications to the coefficients in equations (13) and (14) by the following discussion.

For an airfoil placed in a stationary medium, the equations of motion in dimensional form are shown below after neglecting the aerodynamics terms in the equations given by Fung (1969):

$$\begin{aligned} mh'' + S\alpha'' + C_h h' + K_h(h + \beta_h h^3) &= P(t), \\ Sh'' + I_\alpha \alpha'' + C_\alpha \alpha' + K_\alpha(\alpha + \beta_\alpha \beta^3) &= Q(t). \end{aligned} \tag{30}$$

These represent the equations for a two-degree-of-freedom system with inertia coupling. Since $U = 0$, equations (30) can be reduced to (1) and (2) by defining a nondimensional time $\tau = t/T$ to replace equation (3) where T is a reference time. By re-defining equation (5) to be $U^* = 1/T\omega_\alpha$ and retaining the previous nondimensional parameters, equations (13) and (14) can be used in place of (30) by setting $c_0 = 1$, $c_1 = x_\alpha$, $c_2 = 2\zeta_\xi \bar{\omega}/U^*$, $c_4 = (\bar{\omega}/U^*)^2$, $c_5 = (\bar{\omega}/U^*)^2\beta_\xi$, $c_3 = c_6 = c_7 = c_8 = c_9 = c_{10} = 0$, $d_0 = x_\alpha/r_\alpha^2$, $d_1 = 1$, $d_2 = 2\zeta_\alpha/U^*$, $d_3 = 1/U^{*2}$, $d_4 = \beta_\alpha/U^{*2}$, $d_5 = d_6 = d_7 = d_8 = d_9 = d_{10} = 0$. We note that ω is a nondimensional frequency and is related to the dimensional frequency by

$$\omega = \frac{\Omega}{U^*\Omega_\alpha}, \tag{31}$$

where Ω_α is the pitch natural frequency.

3.1. One-Degree-of-Freedom Dynamic System

For the sake of completeness, we give a brief discussion of a one-degree-of-freedom system when the aerodynamics terms in equations (1) and (2) are neglected. Most of the material found in this section is given by detail by Jones & Lee (1985). If x_α is set equal to zero in equations (1) and (2), the system can be decoupled and the resulting equations to be solved are those for a simple one-degree-of-freedom vibration system with a cubic nonlinearity. For example, if we consider the α degree-of-freedom motion, we can write equation (2) in the form of a Duffing's equation:

$$\alpha'' + c\alpha' + k\alpha + \beta\alpha^3 = F\sin(\omega\tau). \tag{32}$$

Neglecting the damping term $c\alpha'$, Duffing derived the following relation between the amplitude R and the frequency ω for the above nonlinear equation (Stoker 1950):

$$\omega^2 = k + \tfrac{3}{4}\beta R^2 - \frac{F}{R}, \tag{33}$$

which relates ω to the amplitude R of the oscillation. Equation (33) is an interesting relation in that, for certain values of the parameters, there are three values of R associated with one value of ω. This gives rise to a jump phenomenon in which the solution jumps from one branch of the amplitude–frequency curve to another. A first-order expansion can also be developed for equation (32) which includes the damping term $c\alpha'$. This yields (Mickens 1981)

$$\omega^2 = 1 + \tfrac{3}{4}\beta R^2 \pm \frac{F}{R}\left[1 - \frac{c^2R^2}{F^2}\right]^{1/2}, \tag{34}$$

where we have assumed that the linear coefficient, k, is equal to 1. From equation (34) we observe that

$$|R| \leq F/c, \tag{35}$$

where F is assumed positive. Jones & Lee (1985) used the method of Kryloff & Bogoliuboff (1947) and obtained a more accurate amplitude–frequency relation, as follows:

$$\omega^2 = 1 + \tfrac{3}{4}\beta R^2 - \frac{c^2}{2} \pm \frac{F}{R}\left[1 - \frac{c^2R^2}{F^2}\left(1 + \tfrac{3}{4}\beta R^2 - \frac{c^2}{4}\right)\right]^{1/2}, \tag{36}$$

from which an upper limit for R can be found, namely

$$R^2 = -\frac{2}{3\beta}\left(1 - \frac{c^2}{4}\right) \pm \left[\frac{4}{9\beta^2}\left(1 - \frac{c^2}{4}\right)^2 + \frac{4F^2}{3\beta c^2}\right]^{1/2}, \tag{37}$$

in which the + sign is used for $\beta > 0$.

Comparisons of the maximum amplitude given by equations (35) and (37) differ significantly in the case studied by Jones & Lee (1985) and the estimate from equation (35) can be grossly misleading.

It should be noted that these approximations do not yield any information about the effect of initial conditions on the final solution after the transients have died down. In other words, the effect of the initial conditions which determines the branch of the jump where the solution lies is not clear from the analytical studies. Only numerically can we assess the effect of the initial conditions.

To study the behaviour of equation (32) we choose for our model the constants

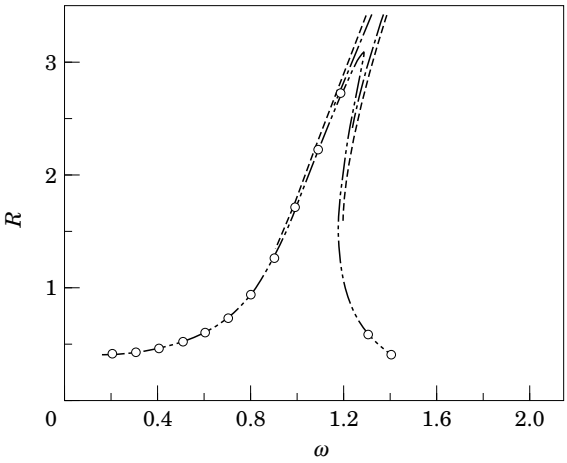

Figure 2. Response curves for Duffing's equation: – – –, equation (33); – · -, equation (34); – · · –, equation (36); ○, numerical, $\alpha(0) = 2{\cdot}0$.

$c = 0{\cdot}1$, $k = 1$, $\beta = 0{\cdot}1$ and $F = 0{\cdot}4$. This corresponds to the following airfoil parameters in equation (2): $\zeta_\alpha = 0{\cdot}05$, $U^* = 1$, $\beta_\alpha = 0{\cdot}1$ and $F = 0{\cdot}4$. The response curve R versus ω is shown in Figure 2 for $0{\cdot}2 \leq \omega \leq 1{\cdot}4$ and in Figure 3 for $1{\cdot}18 \leq \omega \leq 1{\cdot}38$. In the latter case we observe more clearly bending over the response curve to the right. It can be seen that the approximation (36) obtained using the Kryloff & Bogoliuboff method is much more accurate than formula (34) in the region about the peak at $R = 3$. Also shown is Duffing's approximation based on zero damping ($c = 0$).

The numerical simulations were performed using Houbolt's (1950) scheme. The details of the finite-difference time-marching technique are given by Jones & Lee (1985). Our experience in generating the response curve showed that steady-state solutions were obtained in typically 10–40 cycles of period $2\pi/\omega$. Away from the nonunique parts of the curve, i.e. $\omega \leq 1{\cdot}18$ and $\omega \geq 1{\cdot}31$, solutions were obtained with fewer iterations. In the range $1{\cdot}18 < \omega < 1{\cdot}31$ the branch of the response curve on which the solution lies depends upon the initial conditions $\alpha(0)$ and $\alpha'(0)$. For instance, with $\alpha'(0) = 0$ several computations were made with various starting values $\alpha(0)$. With $\alpha(0) = 2$ the jump from the lower branch occurred at about $\omega = 1{\cdot}22$ while with $\alpha(0) = -3{\cdot}5$ the jump occurred at about $\omega = 1{\cdot}32$, as shown on Figure 3.

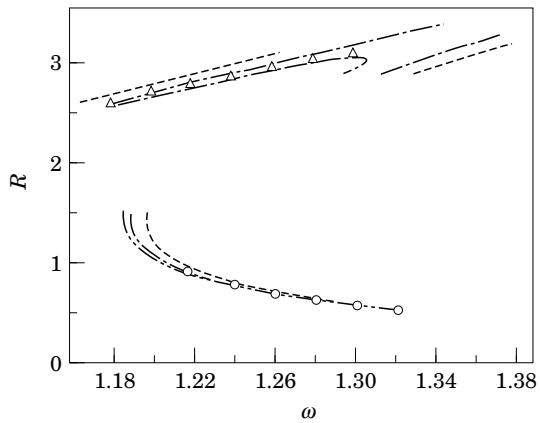

Figure 3. Response curves for Duffing's equation magnified in the jump region: – – –, equation (33); – · -, equation (34); – · · –, equation (36); Δ, numerical, $\alpha(0) = -3{\cdot}5$; ○, numerical, $\alpha(0) = 2{\cdot}0$.

3.2. Two-Degree-of-Freedom Dynamic System

We shall consider two examples to illustrate the complex structure of the jump phenomenon for a two-degree-of-freedom dynamic system with inertia coupling. The coefficients are arbitrary, chosen to generate a set of differential equations for analysis purposes, and they coincide with those equations studied by the authors previously using numerical schemes [for example, Wong *et al.* (1995)]. Other parameters can be used, since the analysis is formulated with only the assumptions that the response is harmonic and the amplitudes are slowly varying functions of time. Hence there should be no limitations to the range of parameters of the system, as long as these assumptions are satisfied. The first example considers the two uncoupled natural frequencies to be equal, while the second examines the case where the frequency separation is fairly large.

3.2.1. *Example I*

The equations studied in this case are

$$\begin{aligned} 0{\cdot}25\alpha'' + \xi'' + 0{\cdot}25\xi' + \xi + 0{\cdot}25\xi^3 &= 0, \\ \alpha'' + 0{\cdot}25\xi'' + 0{\cdot}25\alpha' + \alpha + 0{\cdot}25\alpha^3 &= F\sin(\omega\tau). \end{aligned} \tag{38}$$

The coefficients of these two coupled equations are similar. Following the discussion on equations (30), these expressions can be obtained from (1) and (2) by setting $x_\alpha = 0{\cdot}25$, $r_\alpha = 1$, $U^* = 1$, $\bar{\omega} = 1{\cdot}0$, $\zeta_\alpha = \zeta_\xi = 0{\cdot}125$, $\beta_\alpha = \beta_\xi = 0{\cdot}25$.

To give an indication of the response characteristics for a one-degree-of-freedom system with the given system parameters, we decouple the equations into single degree-of-freedom systems by setting $x_\alpha = 0$. The results thus obtained are used for comparison purposes with the two-degree-of-freedom system. Figure 4 shows the amplitude response curve of $\alpha(\tau)$ against the excitation frequency ω corresponding to $F = 0{\cdot}5$, $1{\cdot}5$ and $3{\cdot}0$, respectively. The results are typical of those for the Duffing equation with different amplitudes of the excitation force (Stoker 1950). It can be verified that the frequency-amplitude relation given in equation (22) is identical to (36) for the one-degree-of-freedom system. For the coupled system governed by equations (38), Figure 5(a, b) shows the amplitude response curves of $\alpha(\tau)$ and $\xi(\tau)$ against the excitation frequency ω for the two-degree-of-freedom system corresponding to $F = 0{\cdot}5$, $1{\cdot}5$ and $3{\cdot}0$. These results were plotted from the relations given in equations

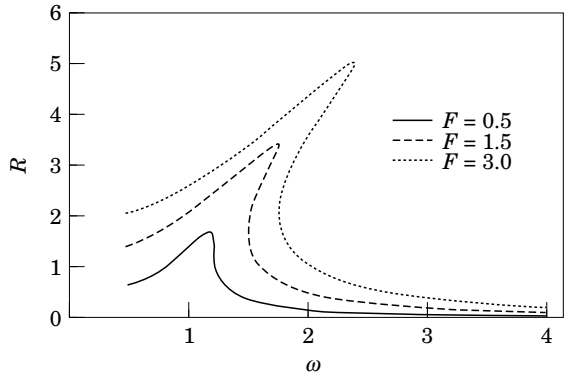

Figure 4. Response curves for different excitation of a one-degree-of-freedom system.

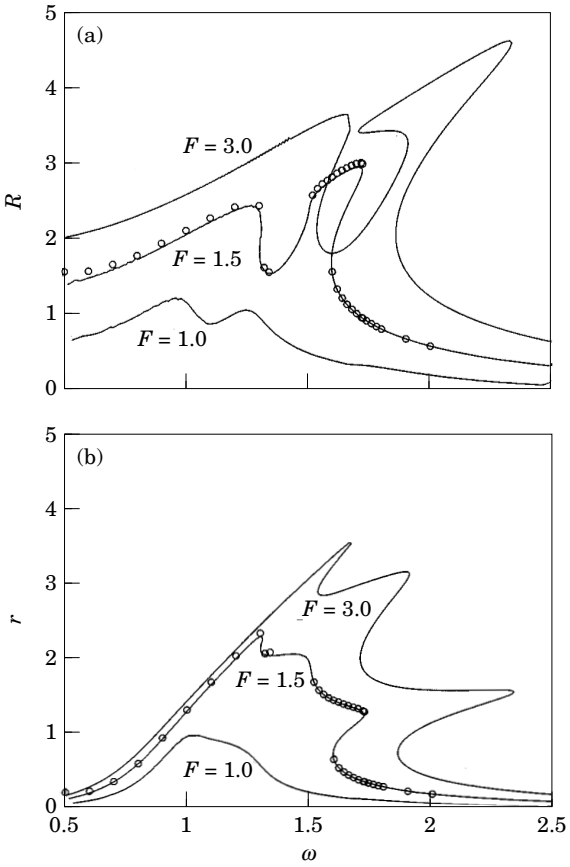

Figure 5. Response of a two-degree-of-freedom system with different excitation: (a) α-response; (b) ξ-response.

(22) and (24). Clearly, the structure of the response curves for the two-degree-of-freedom system is much more complex than that for the one-degree-of-freedom system as F increases. For small values of F, there always exists a harmonic solution in both one and two-degree-of-freedom systems. As F increases, we observe the occurrence of a jump phenomenon and multi-valued amplitude-frequency relations in both systems. Another interesting result noted here is that unlike a one-degree-of-freedom system, we found that for a particular F and for certain values of ω, there may not exist a harmonic solution for the nonlinear system.

The response curve can be divided into various segments where it is possible to identify the existence of harmonic solutions. For example, at $F = 1{\cdot}5$ in Figure 5(a,b) the linear stability analysis given by equation (29) predicts that for $\omega < 1{\cdot}3015$ the system has only one harmonic solution. For $1{\cdot}3015 < \omega < 1{\cdot}3095$, the system has two harmonic solutions and there exists a jump phenomenon in this segment. In the interval (1·3095, 1·3555), the corresponding equilibrium points are stable, but in the interval (1·3555, 1·5038), harmonic solution is not possible. This interval decreases as $\bar{\omega}$ moves away from unity. Some preliminary studies by computing the eigenvalues of the fixed points of Poincaré maps show that there exists two Hopf bifurcations at $\omega = 1{\cdot}3555$ and 1·5038. The solutions for $1{\cdot}3555 < \omega < 1{\cdot}5038$ appear to be quasiperiodic, but more detailed results confirming this observation will appear in a later paper. For $1{\cdot}5038 < \omega < 1{\cdot}595$, a harmonic solution is found and increasing ω to the interval

(1·595, 1·7234), a second jump phenomenon occurs. For $\omega > 1{\cdot}7234$, only harmonic solutions are predicted.

These observations are confirmed by numerical integration of the equations of motion and are represented by the open circles in the figure for $F = 1{\cdot}5$. When $F = 3{\cdot}0$, the responses are more complex than those exhibited for $F = 1{\cdot}5$. In addition to failure in reaching harmonic solutions for certain values of ω, we also observe the existence of chaotic motions and subharmonic solutions. However, this case has not be extensively studied both analytically and numerically as in the previous case for $F = 1{\cdot}5$.

3.2.2. *Example II*

In this example, the analytical results are supplemented by results from numerical simulations. The time-marching finite-difference techniques used are an eighth order scheme given by Lee & LeBlanc (1986) and a fourth-order Runge-Kutta technique whereby equations (13) and (14) are expressed in finite difference form. Both methods given the same results.

The equations studied in this case are given as follows:

$$\begin{aligned} \xi'' + 0{\cdot}2\alpha'' + 0{\cdot}8\xi + 0{\cdot}1\xi^3 = 0, \\ 0{\cdot}2\xi'' + \alpha'' + 0{\cdot}1\alpha' + \alpha + 0{\cdot}1\alpha^3 = F\sin(\omega\tau), \end{aligned} \tag{39}$$

and they are obtained from equations (1) and (2) by choosing the parameters $x_\alpha = 0{\cdot}2$, $r_\alpha = 1$, $U^* = 1$, $\bar{\omega}^2 = 0{\cdot}8$, $\zeta_\alpha = 0{\cdot}05$, $\zeta_\xi = 0$, $\beta_\alpha = 0{\cdot}1$, $\beta_\xi = 0{\cdot}125$. Again, it is emphasized that the system parameters are chosen to coincide with a set of different equations that the authors have previously studied and there is no specific significance to the chosen parameters.

Figure 6(a) shows the amplitude response curve r for $\xi(\tau)$ against the excitation frequency ω when $F = 1{\cdot}0$. The corresponding response in the α degree of freedom is given in Figure 6(b) which shows a more complex structure in the jump region. We find that, for $\omega = 1{\cdot}5$, equations (39) have seven equilibrium points. Once these values are computed, the stability can be determined from the sign of the real part of all the eigenvalues evaluated from equation (29). The results are summarized in Table 1. Only three equilibrium points are found to be stable according to the linear stability analysis.

A detailed numerical study was also carried out for this particular example to demonstrate some of the features of the coupled system. The existence of multi-valued harmonic solutions is confirmed by a numerical simulation using equations (13) and (14). Figure 7(a–c) shows three stable harmonic solutions for $\alpha(\tau)$ and $\xi(\tau)$ from the numerical solutions using the following initial conditions:

$$[\alpha(0), \alpha'(0), \xi(0), \xi'(0)] = [-1, 0, 0, 0],$$
$$[\alpha(0), \alpha'(0), \xi(0), \xi'(0)] = [-3, 5, -3, 5],$$
$$[\alpha(0), \alpha'(0), \xi(0), \xi'(0)] = [0, 5, 0, 5].$$

The first set of initial conditions gives a solution on the lower branch of the amplitude–frequency curve, while the second set gives a solution on the upper branch. The third set of initial conditions gives the solution between these two branches. The solid line in the figures denotes the α response while the dashed line denotes the ξ response. Our computational results indicated that the harmonic solutions at the upper branch of the amplitude–frequency response curve are in phase with approximately the same amplitude. On the lower branch, the solutions have different amplitudes and are

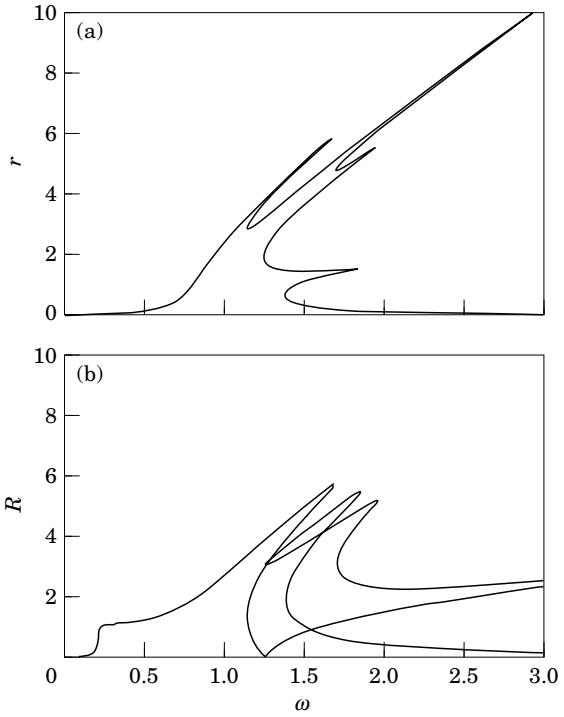

Figure 6. Amplitude response curve of a two-degree-of-freedom system with $F = 1{\cdot}0$: (a) ξ-response; (b) α-response.

180° out of phase. In-between these two branches, the α- and ξ- amplitudes are close to those on the lower and upper branches, respectively. The phase difference between the α and ξ responses is 180°. From our analysis, the analytical solutions (15) can be written as

$$\alpha(\tau) = R\sin(\omega\tau + \phi_1), \qquad \xi(\tau) = r\sin(\omega\tau + \phi_2). \tag{40}$$

Once the values of a_i and b_i are computed, we obtain the amplitudes R and r and the corresponding phase angles. These results are shown in Table 2 and comparison with numerical results shows good agreement.

Phase-space plots of $\alpha'(\tau)$ versus $\alpha(\tau)$ and $\xi'(\tau)$ versus $\xi(\tau)$ were computed and typical plots are given in Figure 8(a–c) for ξ in the lower, upper, and middle branches of the amplitude-frequency response curve. The forcing frequency is $\omega = 1{\cdot}5$. These

TABLE 1
Equilibrium points and signs of Re(λ) for Example II

a_1	b_1	a_2	b_2	Re(λ_1)	Re(λ_2)	Re(λ_3)	Re(λ_4)	Stability
0·042	0·293	−0·135	−0·940	−	−	−	−	Stable
0·559	0·961	−1·686	−2·898	+	+	−	+	Unstable
0·892	−1·127	−2·567	−3·244	+	+	−	−	Unstable
0·494	−4·244	−0·089	0·766	−	−	−	−	Stable
2·023	−3·019	−2·066	3·083	−	+	−	−	Unstable
−3·434	−3·615	−3·162	−3·329	−	−	+	+	Unstable
−3·734	3·362	−3·682	3·315	−	−	−	−	Stable

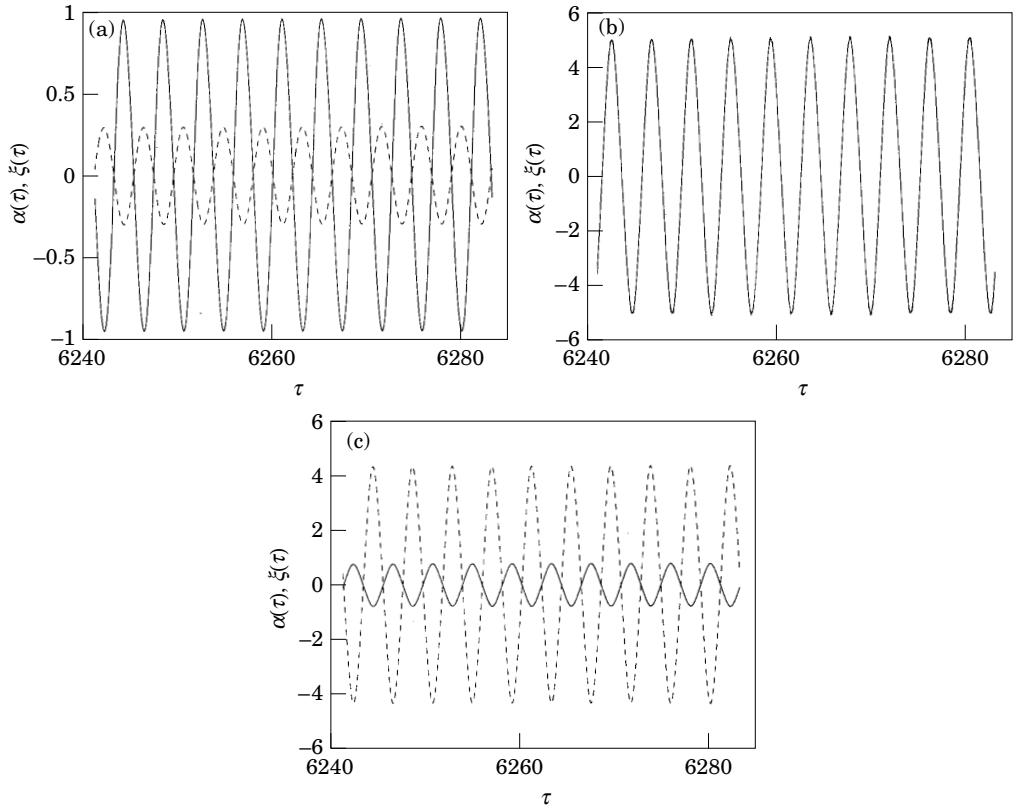

Figure 7. (a) Time series of response on lower branch of jump; (b) time series of response on upper branch of jump; (c) time series of response between upper and lower branches of jump. —, α-response; -----, ξ-response.

figures, and similar ones with different initial conditions that are not included in this paper, show that steady state orbits are reached after the transients have been damped out. The time it takes to reach steady state depends on the initial conditions and the value of the forcing frequency ω.

Power-spectral-density plots are often used to investigate the periodic nature of the system response. A typical power spectral density plot for the ξ degree-of-freedom

TABLE 2

Amplitudes and phases of response for Example II

R Analytic	ϕ_1 (deg) Analytic	r Analytic	ϕ_2 (deg) Analytic	$\phi_1 - \phi_2$ (deg) Analytic	R Numerical	r Numerical	$\phi_1 - \phi_2$ (deg) Numerical
0·9497	8	0·2960	−172	180	0·9510	0·2964	180
3·3528		1·1118					
4·1368		1·4373					
0·7712	174	4·2727	−6	180	0·7727	4·3283	180
3·7112		3·6341					
4·5913		4·9860					
4·9544	−48	5·0245	−48	0	5·0262	5·0972	0

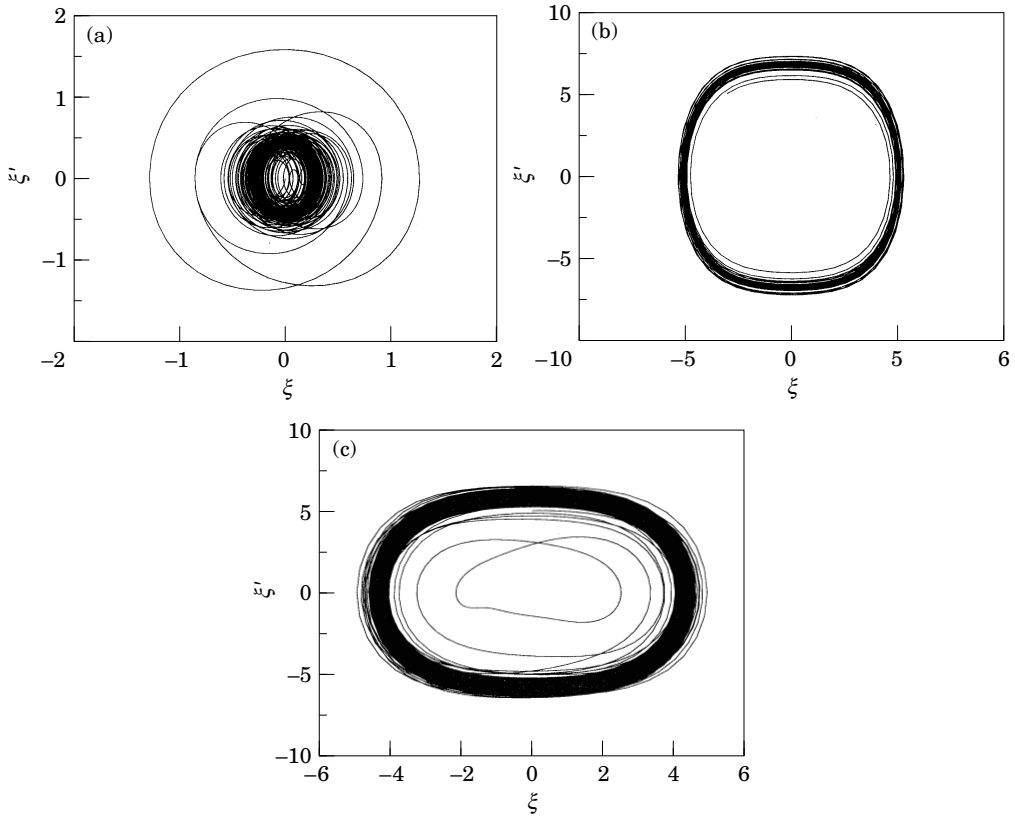

Figure 8. (a) ξ-response on the lower branch of jump; (b) ξ-response on the upper branch of jump; (c) ξ-response between upper and lower branches of jump.

motion at $\omega = 1{\cdot}5$ is given in Figure 9. This figure clearly shows periodic motion, with the fundamental harmonic at least three orders of magnitude higher than the second harmonic. Notice that the harmonics with frequencies 3ω and 5ω observed in the figures can be directly obtained from expanding α^3 and ξ^3 using equations (18). The assumption made in the theoretical analysis that higher harmonics can be neglected appears to be well justified in this example.

3.3. An Example in Aeroelasticity for a Two-Degree-of-Freedom System

To investigate the effects of aerodynamics in equations (13) and (14), we use the same airfoil parameters as those in Example II and choose $a_h = -\frac{1}{2}$ and $\mu = 25$. This corresponds to a light airfoil whose elastic axis is placed at the $\frac{1}{4}$-chord point. There is no particular significance to the choice of this airfoil configuration. Other values of a_h and μ can be used, since there are no restrictions on the parameters in the analysis. In order for the linear aerodynamics to be valid, the value of the forcing function F is kept small, so that the pitch angle is less than 15° while at the same time the plunge motion ξ is within the range for equations (7)–(9) to be applicable. These values are chosen assuming the airfoil thickness-ratio is small, and the profile permits attached flow in a cycle of oscillation. Using these airfoil parameters, we first determine the linear flutter speed obtained by setting the nonlinear stiffness terms to be zero. Its

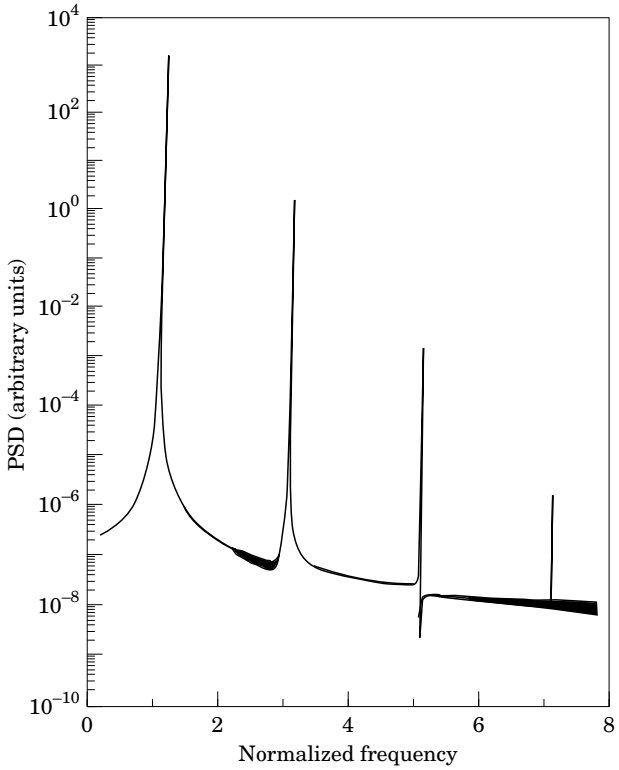

Figure 9. Power spectral density for ξ-response.

value U_L is found to be 2·423. Two values of U^* will be investigated, one at 41% and the other at 95% of U_L, that is, $U^* = 1$ and 2·3019.

The ξ- and α-amplitude-frequency curves are given in Figure 10(a, b), where the amplitude ratios r and R are shown for $U^* = 1$ and $F = 0{\cdot}03$. The units of R are degrees. This value of excitation is chosen in order that the linear aerodynamics theory can be expected to be valid. The case without consideration of aerodynamics is shown in Figure 11(a, b). Both sets of figures show the presence of two peaks at ω approximately 0·86 and 1·07. These frequencies can be estimated from equations (13) and (14). By decoupling the two equations, we can show that $\omega_\alpha = 1/U^*$ and $\omega_\xi = \omega_\alpha \bar{\omega}$ by definition. Since $U^* = 1$ and $\bar{\omega}^2 = 0{\cdot}8$ in this example, we obtain $\omega_\xi = 0{\cdot}89$ and $\omega_\alpha = 1$ which are close to the observed values in the figures. It is interesting to see that the aerodynamic forces decrease the amplitude of the ξ-mode, while the α-mode remains relatively unchanged. The numerical simulation results are also included in the figures and they are denoted by the open circles. It is seen that good agreement is obtained. Comparison with Figure 6(a, b) shows that the complex jump condition is not encountered. However, when the forcing amplitude F is increased to larger values, these jumps are also detected for the nonaerodynamic case. No computations were carried out with aerodynamic forces included since the linear aerodynamics assumptions are violated.

Increasing U^* to 0·95 U_L shows the disappearance of one of the modes [Figure 12(a, b)]. It is seen from this figure that the peak occurs at $\omega \approx 0{\cdot}43$. For the uncoupled modes, the natural frequencies ω_α and ω_ξ are estimated to be 0·4344 and 0·3885,

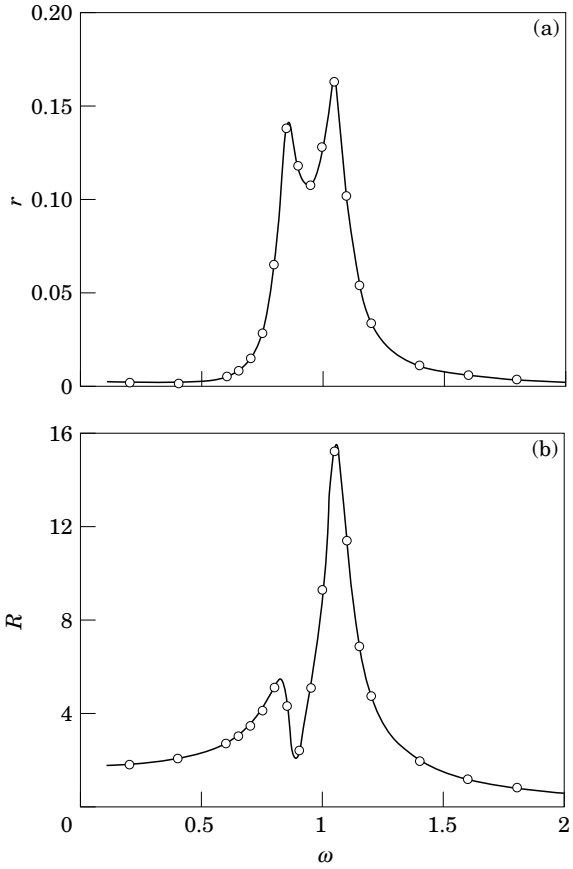

Figure 10. Amplitude response curve of a two-degree-of-freedom system for $\mu = 25$, $U^* = 1$ in a moving medium: (a) ξ-response; (b) α-response.

respectively, for $U^* = 2{\cdot}3019$ and $\bar{\omega}^2 = 0{\cdot}8$. The forcing amplitude in this case is $F = 0{\cdot}002$, which is very small. However, this is expected since only a weak external forcing to the airfoil is required in order to maintain a harmonic motion of sufficiently large amplitude as the linear flutter speed is approached. Also, near the flutter boundary, coalesence of the two modes accounts for the observation of only one peak in Figure 12(a, b).

Comparison of Figure 11(a, b) with 13(a, b) shows the shapes of the response curves to be similar, except for the locations of the peaks and their amplitudes. The dimensional frequency ratio Ω/Ω_α is actually the same since, in the form given as ω, it is scaled by a factor of U^* as shown in equation (31). The differences in amplitude are due to the value of the forcing F which decreases from 0·03 to 0·002. In Figure 12(a), the peak location when expressed in ratio of dimensional frequencies is 0·9898, which is close to the pitch frequency in Figure 10(a). In these two examples, multiple values are not predicted for these values of F. The solution is harmonic, and the stability analysis shows all real parts of λ in equation (21) to be negative.

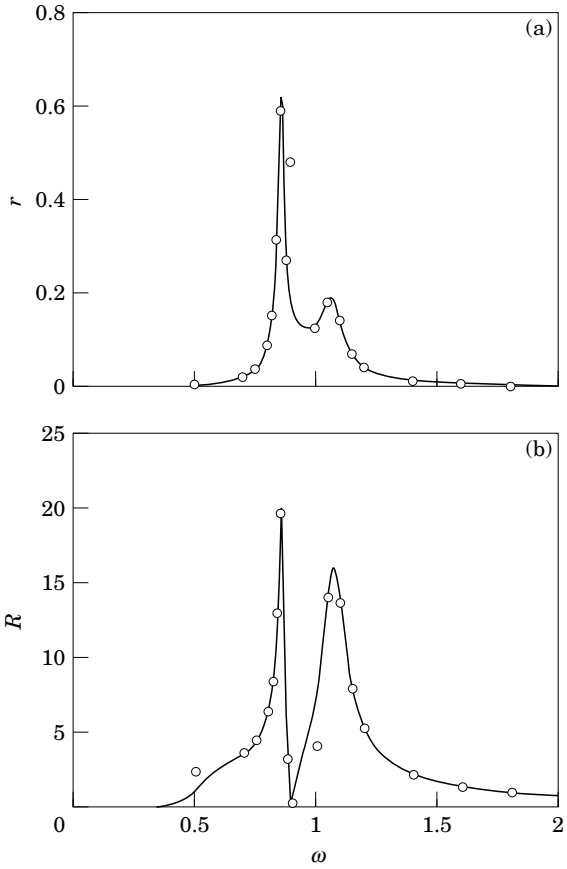

Figure 11. Amplitude response curve of a two-degree-of-freedom system for $\mu = 25$, $U^* = 1$ in a stationary medium: (a) ξ-response; (b) α-response.

4. CONCLUDING REMARKS

In this paper, we investigate the dynamic response of a coupled two-degree-of-freedom system with a cubic nonlinearity in the restoring force. The system chosen for our model is a two-dimensional airfoil oscillating in pitch and in plunge. The equations formulated can readily be adapted to nonaeronautical systems by neglecting the aerodynamics terms and setting the parameters to correspond to those for the particular system under consideration. The analysis provides a technique to determine the amplitude–frequency relation and also to analyse the stability of the equilibrium points. The results were obtained subject to the assumptions that higher harmonics in the response are small and the amplitudes are slowly varying functions of time, such that the second time-derivatives can be neglected. Examples in one- and two-degree-of-freedom systems with various parameters are given. These assumptions are found to be valid for the examples given from the excellent agreement with numerical simulation results. It is found that the amplitude–frequency response curve for a two-degree-of-freedom system has a much more complex structure compared to that for a one-degree-of-freedom system. This is not surprising, since the amplitude-frequency relation can be described by a cubic equation for a one-degree-of-freedom system; whereas it becomes a polynomial of degree 11 for a two-degree-of-freedom system.

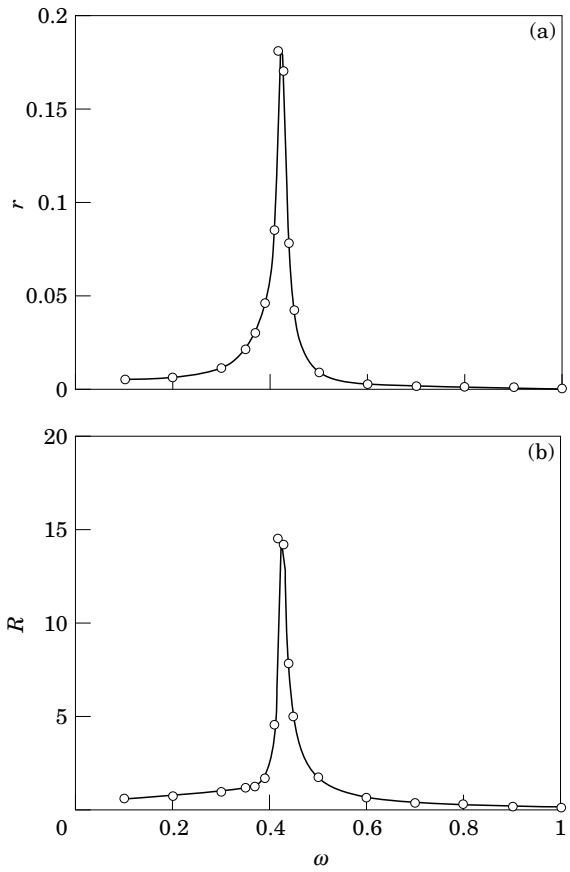

Figure 12. Amplitude response curve of a two-degree-of-freedom system for $\mu = 25$, $U^* = 0{\cdot}95U_L$ in a moving medium: (a) ξ-response; (b) α-response.

Another interesting result observed in the examples studied is that for a two-degree-of-freedom system, harmonic solutions may not exist for certain values of the system parameters. However, in those cases where harmonic solutions are found, the accuracy of the analysis is verified by numerical integration of the exact equations that shows good agreement between the theoretical results and numerical computations.

The application of the analysis to aeroelasticity is demonstrated by an example. Only the effect of velocity is studied, and the response characteristics to variations in airfoil parameters have not been carried out, although such a study is rather straightforward, using the analytical formulation. The use of linear aerodynamics restricts the amplitudes of the plunge and pitch motions to be small. For this reason, the complex jump phenomenon predicted for dynamic systems in a stationary medium with large forcing is not observed. It is shown in the example that two peaks in the response curves are observed at low velocities. As the velocity increases and approaches the linear flutter speed, only one peak is detected. This is a common observation in aeroelasticity when binary flutter occurs.

ACKNOWLEDGEMENTS

The authors gratefully acknowledge the financial support of the NSERC of Canada.

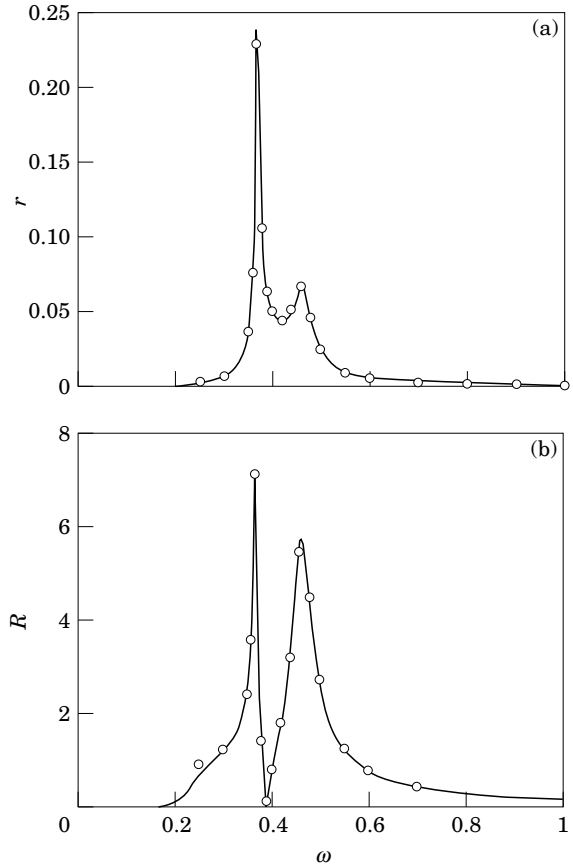

Figure 13. Amplitude response curve of a two-degree-of-freedom system for $\mu = 25$, $U^* = 0{\cdot}95U_L$ in a stationary medium: (a) ξ-response; (b) α-response.

References

Bisplinghoff, R. L., Ashley, H. & Halfman, R. L. 1995 *Aeroelasticity.* Cambridge, Mass: Addison-Wesley Publishing.

Fung, Y. C. 1969 *An Introduction to the Theory of Aeroelasticity.* New York: Dover Publications.

Houbolt, J. C. 1950 A recurrence matrix solution for the dynamic response of elastic aircraft. *Journal Aeronautical Sciences* **17,** 540–550.

Jones, D. J. & Lee, B. H. K. 1985 Time marching numerical solution of the dynamic response of nonlinear systems. National Research Council of Canada, NAE-AN-25, NRC No. 24131.

Jones, R. T. 1940 The unsteady lift of a wing of finite aspect ratio. NACA Report 681.

Jordan, D. W. & Smith, P. 1983 *Nonlinear Ordinary Differential Equations.* Oxford: Clarendon Press.

Kryloff, N. & Bogoliuboff, N. 1947 *Introduction to Nonlinear Mechanics,* Translation by Solomon Lifschitz. Princeton: Princeton University Press.

Lee, B. H. K. & Leblanc, P. 1986 Flutter analysis of a two-dimensional airfoil with cubic non-linear restoring force. National Research Council of Canada, NAE-AN-36, NRC No. 25438.

Lee, B. H. K. & Desrochers, J. 1987 Flutter analysis of a two-dimensional airfoil containing structural nonlinearities. National Research Council of Canada, LR-618, NRC No. 27833.

Mickens, R. E. 1981 *An Introduction to Nonlinear Oscillations.* Cambridge: Cambridge University Press.

Popov, E. P. 1957 On the use of the harmonic linearization method in automatic control theory. NACA TM 1406.

Price, S. J., Lee, B. H. K. & Alighanbari, H. 1994 Post-instability behavior of a two-dimensional airfoil with a structural nonlinearity. *Journal of Aircraft* **31,** 1395–1401.

PRICE, S. J., ALIGHANBARI, H. & LEE, B. H. K. 1995 The aeroelastic response of a two-dimensional airfoil with bilinear and cubic structural nonlinearities. *Journal of Fluids and Structures* **9,** 175–193.

SHEN, S. F. 1959 An approximate analysis of nonlinear flutter problems. *Journal of Aeronautical Sciences* **26,** 25–32.

STOKER, J. J. 1950 *Nonlinear Vibrations.* New York: Interscience Publishers.

WONG, Y. S., LEE, B. H. K. & GONG, L. 1995 Dynamic response of a two-degree-of-freedom system with a cubic nonlinearity. *Third International Conference on Computational Physics,* Chung-Li, Taiwan; to appear in the *International Journal of Modern Physics* **6,** Singapore: World Scientific Publishers.

WOOLSTON, D. S., RUNYAN, H. L. & ANDREWS, R. E. 1957 An investigation of certain types of structural nonlinearities on wing and control surface flutter. *Journal of Aeronautical Sciences* **24,** 57–63.

APPENDIX A: COEFFICIENTS IN EQUATIONS (13) AND (14)

$$c_0 = 1 + \frac{1}{\mu}, \qquad c_1 = x_\alpha - \frac{a_h}{\mu}, \qquad c_2 = 2\zeta_\xi \frac{\bar{\omega}}{U^*} + \frac{2}{\mu}(1 - \psi_1 - \psi_2),$$

$$c_3 = \frac{1 + 2(1/2 - a_h)(1 - \psi_1 - \psi_2)}{\mu}, \qquad c_4 = \left(\frac{\bar{\omega}}{U^*}\right)^2 + \frac{2}{\mu}(\psi_1\epsilon_1 + \psi_2\epsilon_2), \qquad c_5 = \left(\frac{\bar{\omega}}{U^*}\right)^2 \beta_\xi,$$

$$c_6 = \frac{2}{\mu}\{(1 - \psi_1 - \psi_2) + (\tfrac{1}{2} - a_h)(\psi_1\epsilon_1 + \psi_2\epsilon_2)\}, \qquad c_7 = \frac{2}{\mu}\psi_1\epsilon_1\{(1 - (\tfrac{1}{2} - a_h)\epsilon_1)\}$$

$$c_8 = \frac{2}{\mu}\psi_2\epsilon_2\{(1 - (\tfrac{1}{2} - a_h)\epsilon_2)\}, \qquad c_9 = -\frac{2}{\mu}\psi_1\epsilon_1^2, \qquad c_{10} = -\frac{2}{\mu}\psi_2\epsilon_2^2;$$

$$f(\tau) = \frac{2}{\mu}((\tfrac{1}{2} - a_h)\alpha(0) + \xi(0))(\psi_1\epsilon_1 e^{-\epsilon_1\tau} + \psi_2\epsilon_2 e^{-\epsilon_2\tau});$$

$$d_0 = \frac{x_\alpha}{r_\alpha^2} - \frac{a_h}{\mu r_\alpha^2}, \qquad d_1 = 1 + \frac{1 + 8a_h^2}{8\mu r_\alpha^2}, \qquad d_2 = 2\frac{\zeta_\alpha}{U^*} + \frac{1 - 2a_h}{2\mu r_\alpha^2} - \frac{(1 + 2a_h)(1 - 2a_h)(1 - \psi_1 - \psi_2)}{2\mu r_\alpha^2},$$

$$d_3 = \frac{1}{U^{*2}} - \frac{1 + 2a_h}{2\mu r_\alpha^2} - \frac{(1 + 2a_h)(1 - 2a_h)(\psi_1\epsilon_1 + \psi_2\epsilon_2)}{2\mu r_\alpha^2}, \qquad d_4 = \frac{\beta_\alpha}{U^{*2}},$$

$$d_5 = -\frac{(1 + 2a_h)(1 - \psi_1 - \psi_2)}{\mu r_\alpha^2}, \qquad d_6 = -\frac{(1 + 2a_h)(\psi_1\epsilon_1 + \psi_2\epsilon_2)}{\mu r_\alpha^2},$$

$$d_7 = -\frac{(1 + 2a_h)\psi_1\epsilon_1[1 - (1/2 - a_h)\epsilon_1]}{\mu r_\alpha^2}, \qquad d_8 = -\frac{(1 + 2a_h)\psi_2\epsilon_2[1 - (1/2 - a_h)\epsilon_2]}{\mu r_\alpha^2},$$

$$d_9 = \frac{(1 + 2a_h)\psi_1\epsilon_1^2}{\mu r_\alpha^2}, \qquad d_{10} = \frac{(1 + 2a_h)\psi_2\epsilon_2^2}{\mu r_\alpha^2}; \qquad g(\tau) = -\frac{(1 + 2a_h)f(\tau)}{2r_\alpha^2} + F\sin(\omega\tau).$$

APPENDIX B: COEFFICIENTS IN EQUATIONS (20)

$$y_1(x) = (c_0\omega^2 - c_4 - \tfrac{3}{4}c_5r^2)a_1 - c_2\omega b_1 + (c_1\omega^2 - c_6)a_2 - c_3\omega b_2 - c_7a_3 - c_8a_4 - c_9a_5 - c_{10}a_6,$$

$$y_2(x) = c_2\omega a_1 + (c_0\omega^2 - c_4 - \tfrac{3}{4}c_5r^2)b_1 + c_3\omega a_2 + (c_1\omega^2 - c_6)b_2 - c_7b_3 - c_8b_4 - c_9b_5 - c_{10}b_6,$$

$$y_3(x) = (d_0\omega^2 - d_6)a_1 - d_5\omega b_1 + (d_1\omega^2 - d_3 - \tfrac{3}{4}d_4R^2)a_2 - d_2\omega b_2 - d_7a_3 - d_8a_4 - d_9a_5 - d_{10}a_6,$$

$$y_4(x) = F - [-d_5\omega a_1 + (-d_0\omega^2 + d_6)b_1 - d_2\omega a_2 - (d_1\omega^2 - d_3 - \tfrac{3}{4}d_4R^2)b_2 + d_7b_3 + d_8b_4 + d_9b_5 + d_{10}b_6],$$

$$y_5(x) = a_2 - \epsilon_1a_3 - \omega b_3, \qquad y_6(x) = b_2 - \epsilon_1b_3 + \omega a_3, \qquad y_7(x) = a_2 - \epsilon_2a_4 - \omega b_4,$$

$$y_8(x) = b_2 - \epsilon_2b_4 + \omega a_4, \qquad y_9(x) = a_1 - \epsilon_1a_5 - \omega b_5, \qquad y_{10}(x) = b_1 - \epsilon_1b_5 + \omega a_5,$$

$$y_{11}(x) = a_1 - \epsilon_2a_6 - \omega b_6, \qquad y_{12}(x) = b_1 - \epsilon_2b_6 + \omega a_6.$$

APPENDIX C: COEFFICIENTS IN EQUATIONS (21)

$$m_1 = c_2\omega - \frac{c_9\omega}{\epsilon_1^2+\omega^2} - \frac{c_{10}\omega}{\epsilon_2^2+\omega^2}, \qquad n_1 = c_3\omega - \frac{c_7\omega}{\epsilon_1^2+\omega^2} - \frac{c_8\omega}{\epsilon_2^2+\omega^2},$$

$$p_1 = \frac{c_9\epsilon_1}{\epsilon_1^2+\omega^2} + \frac{c_{10}\epsilon_2}{\epsilon_2^2+\omega^2} + c_4 - c_0\omega^2, \qquad q_1 = \frac{3}{4}c_5, \qquad s_1 = c_6 - c_1\omega^2 + \frac{c_7\epsilon_1}{\epsilon_1^2+\omega^2} + \frac{c_8\epsilon_2}{\epsilon_2^2+\omega^2},$$

$$m_2 = d_5\omega - \frac{d_9\omega}{\epsilon_1^2+\omega^2} - \frac{d_{10}\omega}{\epsilon_2^2+\omega^2}, \qquad n_2 = d_2\omega - \frac{d_7\omega}{\epsilon_1^2+\omega^2} - \frac{d_8\omega}{\epsilon_2^2+\omega^2},$$

$$p_2 = \frac{d_9\epsilon_1}{\epsilon_1^2+\omega^2} + \frac{d_{10}\epsilon_2}{\epsilon_2^2+\omega^2} + d_6 - d_0\omega^2, \qquad q_2 = \frac{3}{4}d_4,$$

$$s_2 = d_3 - d_1\omega^2 + \frac{d_7\epsilon_1}{\epsilon_1^2+\omega^2} + \frac{d_8\epsilon_2}{\epsilon_2^2+\omega^2}.$$

APPENDIX D: NOMENCLATURE

a_h	nondimensional distance from airfoil mid-chord to elastic axis
b	airfoil semi-chord
C_h	damping coefficient in plunge degree-of-freedom
C_α	damping coefficient in pitch degree-of-freedom
C_L	aerodynamic lift coefficient
C_M	pitching moment coefficient
F	applied force magnitude
h	plunge displacement
I_α	airfoil mass moment of inertia about elastic axis
K_h	spring constant in plunge degree-of-freedom
K_α	spring constant in pitch degree-of-freedom
m	airfoil mass per unit span
P	external force
Q	external moment
R	response amplitude for α
r	response amplitude for ξ
r_α	radius of gyration about elastic axis
S	airfoil static moment about elastic axis
T	reference time
t	time
U	free-stream velocity
U_L	linear flutter speed
U^*	nondimensional velocity
x_α	nondimensional distance from elastic axis to centre of mass
α	pitch angle
β	coefficient of cubic spring
ζ	damping
μ	airfoil–air mass ratio
ξ	nondimensional displacement
τ	nondimensional time
ϕ	Wagner function
Ω	dimensional frequency
ω	nondimensional frequency